# HokB monomerization and membrane repolarization control persister awakening

*Dorien Wilmaerts*[a,b], *Liselot Dewachter*[a,b], *Pieter-Jan De Loose*[a,b], *Celien Bollen*[a,b], *Natalie Verstraeten*[a,b,1], *Jan Michiels*[a,b,1,2]

[a]Center for Microbiology, VIB, Leuven, 3001, Belgium

[b]Centre of Microbial and Plant Genetics, KU Leuven, Leuven, 3001, Belgium

[1]Co-last authors

[2]Lead contact

Running Head: Formation and awakening of HokB-induced persister cells

Corresponding author and lead contact: Jan Michiels, jan.michiels@kuleuven.vib.be

## SUMMARY

Every bacterial population harbors a small subpopulation of so-called persisters that are transiently antibiotic tolerant. These persisters are associated with the recalcitrance of chronic infections as they can recolonize the host after antibiotic removal. Several effectors have been described to induce persistence, yet persister cell awakening is poorly understood. We previously reported that the toxin HokB induces persistence via pore formation, resulting in membrane depolarization and ATP leakage. We now delineate mechanisms responsible for the awakening of HokB-induced persisters. We show that HokB dimerization by the oxidoreductase DsbA is essential for pore formation and peptide stability. Pores are disassembled via DsbC-mediated monomerization, which targets HokB for DegQ-mediated degradation. Finally, pore disassembly allows membrane repolarization by the electron transport chain, supporting cells to resume growth. Combined, these results provide a detailed view of both formation and awakening of HokB-induced persister cells.

## GRAPHICAL ABSTRACT

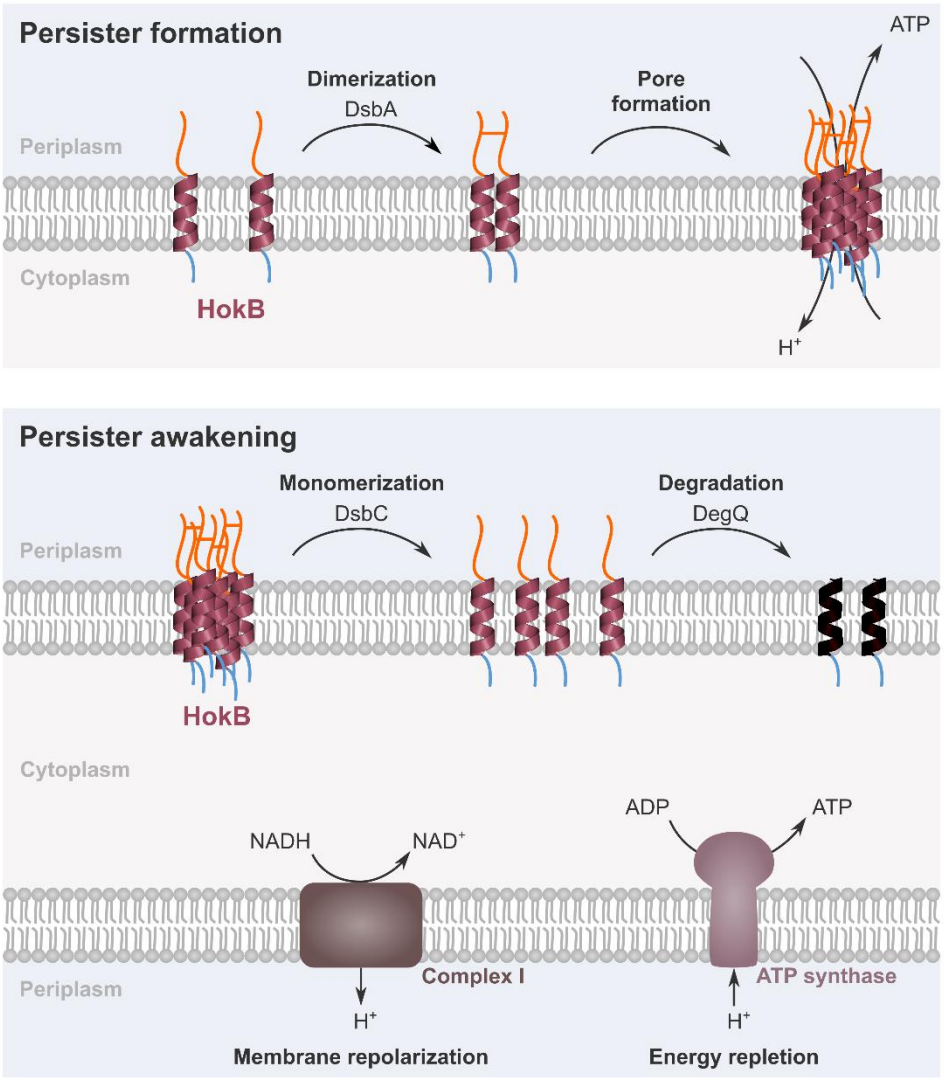


## INTRODUCTION

Bacterial populations harbor a small fraction of persister cells that display transient tolerance to antibiotics (Michiels et al. 2016). These persisters are genetically indistinguishable from sensitive cells within the population and survive antibiotic treatment as a result of phenotypic bistability. Persisters are generally assumed to be in a slow-growing or dormant state, resulting in the inactivity of the antibiotic target (Balaban et al. 2004; Shah et al. 2006). However, the complexity of the persister phenotype likely exceeds target inactivity (Wilmaerts et al. 2019). It was shown that dormancy alone does not evoke the persistence phenotype per se (Orman and Brynildsen 2013) and stationary phase persisters were found to be metabolically active

(Wilmaerts et al. 2018; Orman and Brynildsen 2015). Additionally, persisters can be damaged by the applied antibiotic (Völzing and Brynildsen 2015; Mok and Brynildsen 2018), indicating that the antibiotic target is active. This heterogeneity of the persister population complicates persistence research (Michiels et al. 2016).

Toxin-antitoxin (TA) modules are associated with the formation of persister cells. Indeed, overexpression of numerous toxins increases the number of persister cells (Verstraeten et al. 2015; Y. Kim and Wood 2010; Cheverton et al. 2016; Dörr, Vulić, and Lewis 2010) and deletion of toxin-encoding genes has been reported to decrease persistence in a select number of cases (Dörr, Vulić, and Lewis 2010; Wang and Wood 2011). TA modules are plasmid-encoded or genomic elements. Generally, plasmid-encoded TA modules play a role in post-segregational killing, while genomic TA modules promote survival in stressful environments and take part in mediating persistence (Page and Peti 2016). Toxin-antitoxin modules have been classified in 6 groups based on the antitoxin's mechanism of toxin inhibition (Page and Peti 2016). While the toxin is typically a protein, the antitoxin can be an RNA molecule (type I and III) or a small protein (type II, IV, V and VI).

To date, type I, type II and type V TA modules have been implicated in persistence. In type I TA modules, the antitoxin binds with the toxin mRNA, preventing translation or triggering degradation. For type II TA modules, the protein antitoxin inhibits the protein toxin via direct binding (Harms et al. 2018). The role of type II TA modules in the formation of persister cells is currently under debate (Harms et al. 2017; Holden and Errington 2018; Goormaghtigh et al. 2018). In type V TA modules, the antitoxin is an RNase that specifically degrades the toxin mRNA (Harms et al. 2018). Toxins inhibit an essential cellular function and are believed to induce persistence when their cellular concentration reaches a certain threshold value (Rotem

et al. 2010). This is achieved via stress-induced upregulation of the whole TA operon, combined with stress-induced degradation of the intrinsically unstable antitoxins or by upregulation of the toxins alone (Keren et al. 2004; Shan et al. 2017; Muthuramalingam, White, and Bourne 2016). In addition, both processes are suggested to happen stochastically (Rotem et al. 2010), although this hypothesis is currently not supported by experimental evidence.

While the induction of persistence by toxins is a well-studied phenomenon, the awakening of toxin-induced persister cells remains puzzling. One awakening strategy has been reported for *Salmonella* persisters induced by the type II toxin TacT. In this specific case, persisters resume growth after expression of the Pth protein (Cheverton et al. 2016). In general, persister cells are believed to revert from the antibiotic-tolerant state stochastically, although environmental conditions are suggested to contribute to persister cell awakening (Jõers, Kaldalu, and Tenson 2010; Dworkin and Shah 2010; Buerger et al. 2012). Upon exit from the persister state, a new population can be formed when antibiotics are removed from the environment (Michiels et al. 2016).

In previous work, we have shown that the conserved and essential GTPase ObgE induces persistence in *Escherichia coli* thereby increasing expression of the type I toxin HokB (Verstraeten et al. 2015). HokB is a small membrane peptide that induces persistence through pore formation, thereby leaking ATP and depolarizing the membrane (Wilmaerts et al. 2018; Verstraeten et al. 2015). The HokB antitoxin *sokB* is an RNA molecule which triggers degradation of *hokB* mRNA upon binding (Gerdes 2016). It has been hypothesized that upon membrane depolarization, the enzymatic activity of RNaseE is reduced. This stabilizes *sokB* mRNA and prevents further HokB synthesis (Gerdes 2016). Although this mechanism might explain why the HokB toxin does not evoke cell death, it does not affect the concentration of

HokB peptides already present in the membrane and, as a consequence, it cannot trigger awakening of HokB-induced persister cells. In general, the mechanisms by which HokB-induced persisters are able to wake up remain enigmatic.

In this study, we identify mechanisms that control HokB pore formation and thereby affect both persister state entry and exit. We show that intermolecular dimerization of HokB peptides via their periplasmic cysteine residues is effectuated by the oxidoreductase DsbA and is essential for peptide stability and pore formation. Furthermore, we demonstrate that the dormancy duration of HokB-induced persister cells is positively correlated with the concentration of HokB peptides. Awakening of HokB-induced persister cells relies on two essential processes. First, the HokB pore is destabilized via peptide monomerization through the periplasmic oxidoreductase DsbC. Subsequently, monomeric HokB is degraded by the DegQ protease. Second, HokB-induced persisters rely on membrane repolarization by complex I of the electron transport chain (ETC) to replenish the energy pool and allow regrowth. This work provides detailed insights into both the induction of persistence and the awakening of persister cells, which might prove useful for the development of anti-persister strategies.

## RESULTS

### HokB dimerization by the periplasmic oxidoreductase DsbA is essential for pore formation

In previous work, we have demonstrated that the pore-forming capacity of HokB is essential for persistence and that membrane depolarization and ATP leakage are hallmarks of HokB pore formation (Verstraeten et al. 2015; Wilmaerts et al. 2018). We wanted to gain mechanistic insight in the formation of HokB pores. As the amino acid sequence of HokB contains three

cysteine residues, we hypothesized that these residues would affect HokB pore formation by forming intermolecular disulfide bridges.

The formation of disulfide bridges between two or more HokB peptides was assessed using a non-reducing western blot. This analysis shows that HokB forms both monomers and dimers (Fig.1A). The HokB peptide contains cysteine residues at position C9, C14 and C46. Computational predictions show that C9 and C14 are localized in the membrane, while C46 is localized in the periplasm (Wilmaerts et al. 2018). The potential contribution of these residues to dimerization was determined using HokB cysteine-to-serine substitution mutants ($HokB_{C9S}$, $HokB_{C14S}$ and $HokB_{C46S}$). First, membrane localization of the mutant peptides was confirmed (Fig. S1A). Second, monomer fractions were quantified (Fig. 1B). Interestingly, $HokB_{C46S}$ does not form dimers, demonstrating that the cysteine in the periplasm is responsible for HokB dimerization by disulfide bridge formation. Lastly, peptide concentrations were determined, showing that the concentration of $HokB_{C46S}$ is lower compared to that of HokB, possibly indicating that the absence of dimerization destabilizes the HokB peptide (Fig.1C).

A persistence assay was performed to assess whether dimerization affects HokB-mediated persistence (Fig. 1D). Furthermore, in the strains expressing the cysteine-to-serine mutant peptides, we measured the membrane potential using $DiBAC_4$ (3), a stain that enters cells with a depolarized membrane (Fig. S1B), and ATP leakage (Fig. 1E). Both $HokB_{C9S}$ and $HokB_{C14S}$ induce persistence, depolarize the membrane and result in ATP leakage. Conversely, $HokB_{C46S}$ does not display these phenotypes, demonstrating that it does not form pores. These results indicate that lack of pore formation results from the absence of dimerization.

Spontaneous disulfide bond formation in the periplasm of *E. coli* proceeds slowly and free thiol groups are vulnerable to detrimental oxidation (Bardwell, McGovern, and Beckwith 1991). Therefore, disulfide bond formation is performed by the periplasmic oxidoreductase DsbA (Depuydt, Messens, and Collet 2011). We assessed whether dimerization of HokB is mediated by DsbA. No HokB peptides were detected in a strain lacking DsbA, indicating that HokB is unstable in a Δ*dsbA* mutant. Accordingly, HokB does not induce persistence in this mutant (Fig. 1F). These data show that the absence of dimerization destabilizes HokB peptides, thereby restraining pore formation and thus the induction of persistence. Using the reducing agent dithiothreitol (DTT), we chemically mimicked the effect of absence of *dsbA*. As expected, upon addition of DTT, we could observe a decrease in HokB-induced persister cells (Fig. S1C). In conclusion, HokB dimerization via the periplasmic C46 residue by DsbA is essential for HokB peptide stability and thus for the induction of persistence through pore formation.

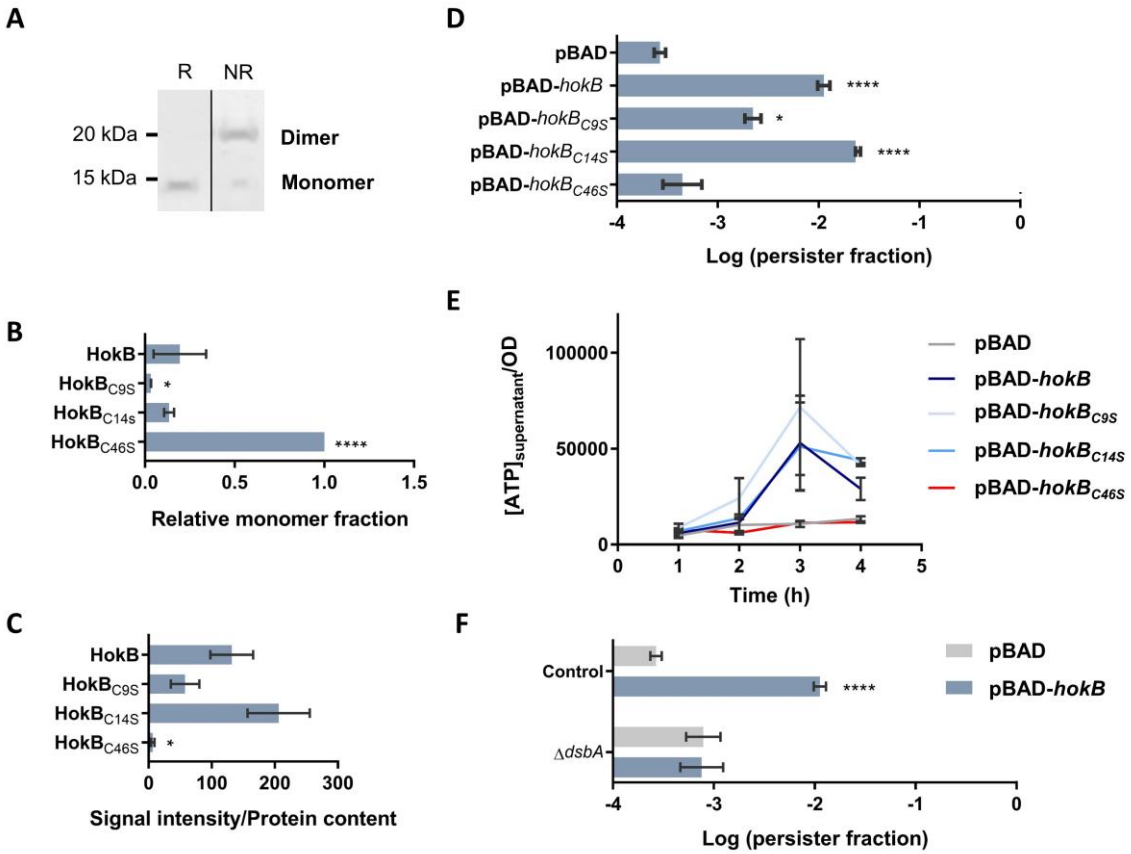

**Figure 1. DsbA forms HokB dimers via the C46 residue.** (A) HokB peptides form dimers that can be visualized on a non-reducing (NR) western blot. Disulfide bridges are broken in a reduced sample (R). Two lanes of the same western blot are shown. (B) A non-reducing western blot was used to quantify monomer fractions, showing that $HokB_{C46S}$ does not form dimers. Values are means ± SEM from at least 3 independent experiments. Asterisks indicate statistical significance compared to HokB (**** $P < 0.0001$; * $P < 0.05$). (C) A reducing western blot was performed to assess HokB peptide concentration. Signal intensities from the band were divided by the total protein concentration of the sample. $HokB_{C46S}$ is unstable compared to HokB. Values are means ± SEM from at least 2 independent experiments. Asterisks indicate statistical significance compared to HokB (* $P < 0.05$). (D) Expression of $hokB_{C46S}$ does not increase the persister fraction, in contrast to $hokB_{C9S}$ and $hokB_{C14S}$. Values are means ± SEM from at least 3 independent experiments. Asterisks indicate statistical significance compared to the empty vector control (**** $P < 0.0001$; * $P < 0.05$). See also Figure S1A and Figure S1B. (E) Expression of *hokB*, $hokB_{C9S}$ and $hokB_{C14S}$ results in ATP leakage, while expression of $hokB_{C46S}$ does not. Values are means ± SEM from at least 3 independent experiments. There is a significant difference ($P < 0.05$) compared to the empty vector control for time point 3 h for $HokB_{C9S}$, $HokB_{C14S}$ and HokB. After 4 h induction, there is a significant difference compared to the empty vector control for $HokB_{C9S}$ ($P < 0.0001$), $HokB_{C14S}$ ($P < 0.0001$) and HokB ($P < 0.05$). (F) Expression of *hokB* in a Δ*dsbA* mutant does not induce persistence. Values are means ± SEM from at least 3 independent experiments. Asterisks indicate statistical significance compared to the empty vector control (**** $P < 0.0001$). See also Fig. S1C.

## Dormancy duration is positively correlated with HokB levels

The previous experiments demonstrate that peptide stability is controlled by DsbA-mediated dimerization via periplasmic C46 residues, which is important for the induction of persistence. To assess whether HokB stability also affects persister cell awakening, we first searched for a potential correlation between the concentration of HokB peptides and awakening of HokB-induced persister cells using two different techniques. Hitherto, it has been challenging in

189 persistence research to directly correlate activity of an effector with persister awakening. Here
190 we took advantage of the fact that HokB is a direct effector of persistence and that its presence
191 can be monitored using a functional mCherry-HokB fusion that effectively induces persistence
192 (Wilmaerts et al. 2018). Furthermore, we were able to measure 73 persisters at the single-cell
193 level, providing increased statistical power compared to previously conducted studies
194 (2,17,26).
195
196 In a first approach, persister cells were loaded in a microfluidic device to record the time to the
197 first cell division. The HokB peptide concentration was measured using the fluorescence
198 intensity of mCherry-HokB. Persister cells were isolated by treating an exponentially growing
199 culture with ceftazidime, lysing the sensitive cells but leaving the persister cells unharmed
200 (Orman and Brynildsen 2013). Our results show that the time to the first cell division is
201 correlated significantly with the fluorescence intensity ($P = 0.0485$, $r = 0.4252$) (Fig. 2A). The
202 time to the first cell division varies strongly between individual persister cells, ranging from
203 66 to 275 min, and is normally distributed. These results were confirmed with stationary-phase
204 cells, treated with ofloxacin. Similar to the previous experiment, the time to first cell division
205 correlates with the fluorescence intensity ($P = 0.064$, $r = 0.4015$) (Fig. 2B). Although not
206 statistically significant, the same trend emerges hinting at a correlation between HokB peptide
207 concentration and dormancy duration also in stationary phase. The time to the first cell division
208 is normally distributed and slightly shifted upwards compared to exponential-phase persisters,
209 ranging from 112.3 to 386.2 min. The normality of the distributions indicates that the
210 awakening of HokB-induced persister cells is not a purely stochastically-determined process,
211 but has an intrinsic time-dependence, suggesting that one or several intermediate steps are
212 necessary for the awakening of HokB-persisters (Norman et al. 2015).
213

The microfluidic device allows visualization of HokB-induced persister cells during awakening. After ceftazidime treatment, 22 persisters were visualized. In addition to 3 cells with a normal morphology, we observed 8 elongated cells and 11 enlarged cells, both giving rise to normal-sized progeny (Fig. 2C). These phenotypes likely result from the antibiotic treatment needed to isolate persister cells, as ceftazidime targets primarily penicillin binding protein 3 (Hayes and Orr 1983), and loss of this protein results in elongated cells (Takeuchi et al. 2005). Ceftazidime also targets other penicillin binding proteins (1 and 2), which presumably results in the enlarged phenotype (Sauvage et al. 2008; Hayes and Orr 1983). Following ofloxacin treatment, persisters initially regrew normally. However, in 50 % of the observed events, persisters gave rise to enlarged cells after a few cell divisions. This phenotype was not inheritable, as their progeny was normally sized. These phenotypes might indicate that many of the persister cells we observed were damaged by the applied antibiotic.

In a second approach, HokB-induced persister cells surviving ceftazidime treatment were sorted in a honeycomb plate using fluorescence activated cell sorting (FACS). The plates, containing a maximum of 1 persister cell per well, were incubated in a Bioscreen device that monitors growth by optical density measurement. Fluorescence intensity was measured during sorting. A significant correlation was observed between the lag time of growth resumption and fluorescence intensity ($P = 0.0253$, $r = 0.4148$) (Fig. S2), corroborating the results of the microfluidics assays.

From these three experiments, we conclude that the dormancy duration of HokB-induced persister cells is positively correlated with the concentration of HokB peptides. Thus, stability of the HokB peptides might be of importance not only for the induction of HokB persister cells

but also for their awakening. Therefore, we hypothesized that proteases might be targeting HokB and reduce its stability, thereby contributing to the awakening process.

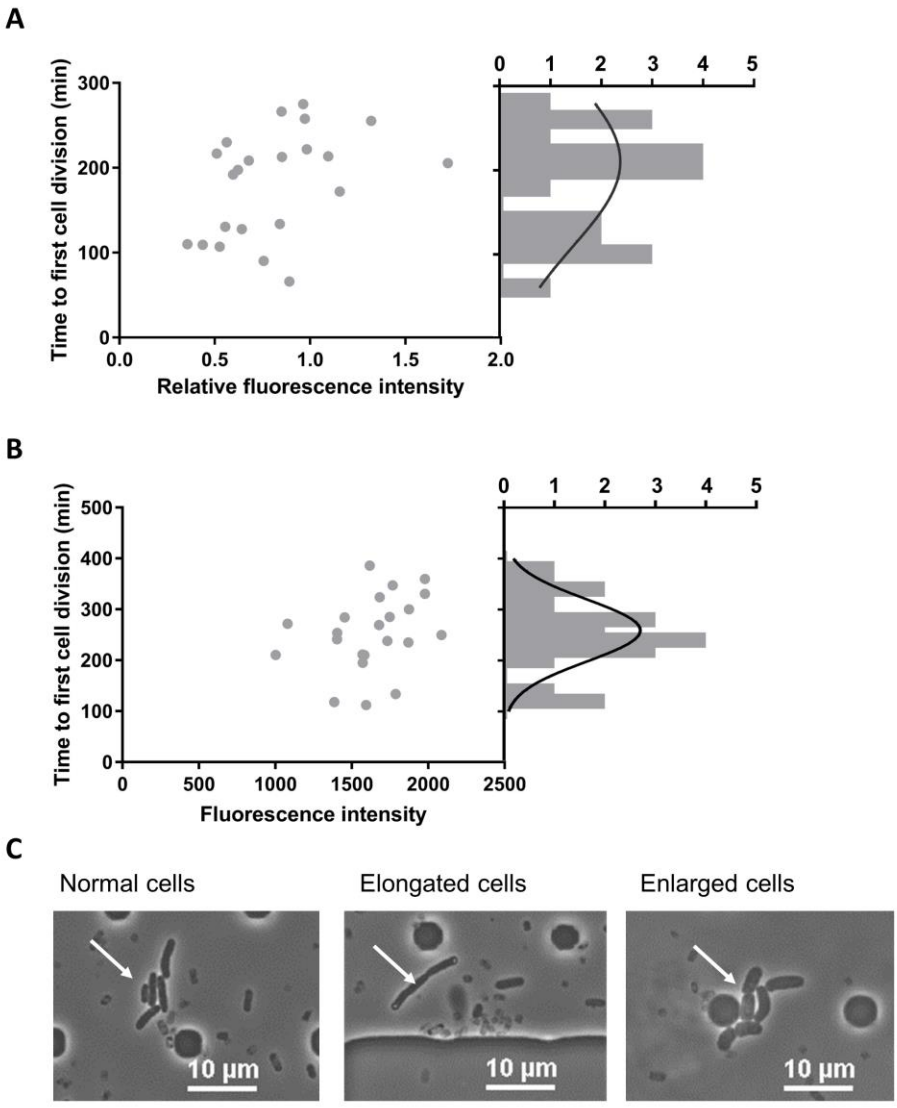


**Figure 2**. **Monitoring persister outgrowth using microfluidics.** (A) Persisters were isolated by treating an exponentially-growing culture with ceftazidime. Upon persister awakening, there is a significant correlation ($P = 0.0485$, $r = 0.4252$) between the number of mCherry-HokB peptides and the time to the first cell division. Spearman correlation was used to assess statistical dependence between the two variables. Normality of the distribution of the time to the first cell division was assessed using the Shapiro-Wilk test. A Gauss curve is plotted on the data, giving an average time to first cell division of 209.8 ± 101 min (mean ± SD). The time to the first cell division varies from 66 min to 275 min. See

also Figure S2. (B) A stationary-phase culture was treated with ofloxacin. Upon persister awakening, there is a correlation (P = 0.064, r = 0.4015) between the number of mCherry-HokB peptides and the time to the first cell division. Spearman correlation was used to assess statistical dependence between the two variables. Normality of the distribution of the time to the first cell division was assessed using the Shapiro-Wilk test. A Gauss curve is plotted on the data, giving an average time to first cell division of 258.7 ± 61.18 min (mean ± SD). The time to first cell division varies from 112.3 min to 386,2 min. (C) Regrowing persister cells have various outgrowth phenotypes. Representative examples are shown.

## HokB is a substrate of the protease DegQ

To identify HokB-degrading proteases, we quantified HokB peptide levels following overexpression of different *E. coli* proteases using the ASKA library (Kitagawa et al. 2005). We selected 5 periplasmic proteases based on their putative function or target (DegP, DegQ, MepA, PtrA, Prc), and as a control two proteases localized in the inner membrane (RseP, FtsH) and three cytoplasmic proteases (ElaD, HslU, HslV). Expression of *degQ, ftsH* and *prc* reduces the concentration of HokB peptides (Fig. S3A), yet only overexpression of *degQ* abolishes HokB-induced membrane depolarization (Fig. S3B). Therefore, further experiments focused on the periplasmic serine protease DegQ. DegQ targets β-branched side chains lacking disulfide bonds (Kolmar, Waller, and Sauer 1996; Waller and Sauer 1996), which is in accordance with computational predictions indicating that the periplasmic part of HokB contains two β strands (Bar-Yaacov et al. 2017) and our observation that HokB monomers are unstable. Using a newly-constructed plasmid that encodes the native DegQ protein, without the 6His-tag present in the ASKA library, we confirmed that overexpression of *degQ* reduces the concentration of HokB peptides by 82% (P = 0.00002) (Fig. 3A) and abolishes HokB-induced membrane depolarization (Fig. 3B). Furthermore, overexpression of *degQ* results in the abolishment of HokB-induced persistence (Fig. 3C). The latter observation is in agreement

with a decreased ATP leakage in a strain that co-expresses both *degQ* and *hokB* for 4 h (Fig. 3D).

To further confirm the role of DegQ, the effect of *degQ* deletion on HokB stability was examined. These experiments show that the concentration of HokB peptides is two-fold higher in a Δ*degQ* mutant compared to the wild-type background (Fig. 3E). However, expression of *hokB* in a Δ*degQ* mutant depolarizes the membrane to the same extent as in the control strain (Fig. 3F). Taken together, our data show that the periplasmic DegQ protease controls the HokB peptide concentration. Deletion of *degQ* reduces the level of HokB-induced persisters three-fold (Fig. 3G). This is surprising, given the higher stability of the peptides and the same number of cells with a depolarized membrane, which would suggest that the number of persisters would be equal. As absence of persister awakening also results in a decreased persister fraction, our data suggest that degradation of HokB by DegQ might play a role in the awakening of HokB-induced persister cells. As DegQ only degrades β-sheets devoid of a disulfide bridge (Kolmar, Waller, and Sauer 1996; Waller and Sauer 1996), we hypothesized that DegQ would not be the only factor at play.

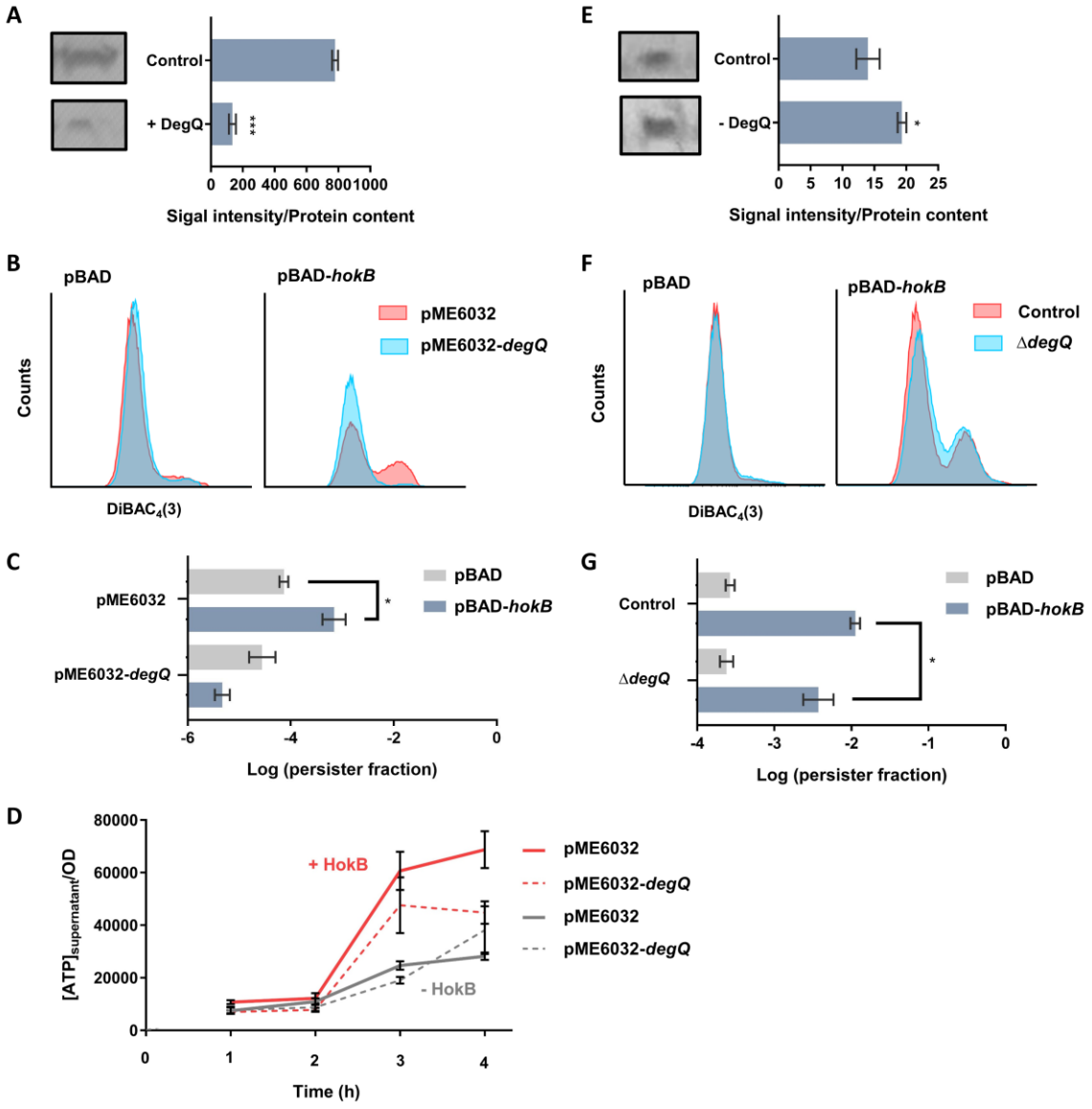


**Figure 3. HokB is a substrate of the periplasmic protease DegQ.** (A) A reducing western blot was performed to assess the HokB peptide concentration. Signal intensities from the band were divided by the total protein concentration of the sample. Expression of *degQ* decreases the concentration of HokB peptides in the population by 82.75 ± 0.02% (mean ± SEM). A representative example of 3 biological repeats is depicted. Values are means ± SEM from at least 3 independent experiments. Asterisks indicate statistical significance (*** $P < 0.0001$). The images shown were obtained from a single western blot. See also Figure S3A. (B) The membrane potential was measured using $DiBAC_4(3)$, showing that HokB does not induce membrane depolarization upon co-expression with *degQ*. A representative example of 3 biological repeats is depicted. See also Figure S3B. (C) Overexpression of *degQ* abolishes HokB-mediated persistence. Values are means ± SEM from at least 3 independent

experiments. Asterisks indicate statistical significance (* $P < 0.05$). (D) Expression of *degQ* results in a decreased concentration of ATP in the supernatant after 4 h induction of both *degQ* and *hokB.* Values are means ± SEM from at least 3 independent experiments. $P < 0.05$ for the comparison of pBAD and pBAD-*hokB* for both PME6032 and PME6032-*degQ* after 3 h induction. $P < 0.05$ for the comparison of pBAD and pBAD-*hokB* for PME6032 after 4 h induction. (E) A reducing western blot was performed to assess the HokB peptide concentration. Signal intensities from the band were divided by the total protein concentration of the sample. HokB peptides are stabilized in a *degQ* deletion mutant. A representative example of 3 biological repeats is depicted. Values are means ± SEM from at least 3 independent experiments. Asterisks indicate statistical significance (* $P < 0.05$). The images shown were obtained from a single western blot. (F) Expression of *hokB* in a *degQ* deletion mutant does not statistically affect the number of cells with a depolarized membrane. (G) *degQ* deletion significantly decreases HokB-mediated persistence. Values are means ± SEM from at least 3 independent experiments. Asterisks indicate statistical significance (* $P < 0.05$).

## HokB degradation requires peptide monomerization by the oxidoreductase DsbC

So far, we have established that HokB peptides are stabilized by DsbA-mediated dimerization and our data suggest that persister awakening relies on degradation of HokB by DegQ. While monomeric HokB peptides are detected in *E. coli* (Fig. 1A and B), the oxidative state of the periplasm impedes reduction of disulfide bonds at a frequent rate, which is a requirement for DegQ to degrade proteins (Kolmar, Waller, and Sauer 1996; Waller and Sauer 1996). An interesting candidate to assist in DegQ-mediated degradation of HokB is DsbC. This oxidoreductase uses electrons originating from NADPH and passed along by the thioredoxin TrxA to reduce disulfide bonds generated by DsbA (Depuydt, Messens, and Collet 2011). We reasoned that DsbC could potentially monomerize HokB peptides. Corroborating this hypothesis, we could not detect any HokB monomers in a strain lacking DsbC (Fig. 4A). Next, we assessed whether monomerization by DsbC is essential for DegQ-mediated degradation of

HokB peptides. For this, HokB and DegQ were co-expressed in a Δ*dsbC* mutant and the concentration of HokB peptides was measured quantitatively (Fig. 4B). As shown before, DegQ significantly reduces HokB peptide levels by more than 80% in a wild-type strain. However, in the absence of DsbC, expression of *degQ* does not significantly reduce HokB levels. This indicates that monomerization of HokB by DsbC is important for DegQ-mediated degradation of HokB.

To assess whether persister levels are altered in a Δ*dsbC* mutant, a persistence assay was performed in this mutant. As expected, HokB does not increase the persister fraction. Interestingly however, expression of *hokB* has a dominant negative effect in the absence of DsbC as it significantly decreases the persister fraction in comparison to a vector control (Fig. 4C). This effect is abolished by addition of the disulfide-reducing compound DTT, indicating that it results from disulfide bridge formation (Fig. S4A). We next sought to identify the origin of this dominant negative effect. Although HokB only possesses a single cysteine residue exposed in the periplasm (C46), it was shown that the tyrosine at position 29 is affected by an adenosine-to-inosine RNA editing system, occasionally resulting in an additional periplasmic cysteine at position 29 (Bar-Yaacov et al. 2017). We reasoned that DsbC might break disulfide bonds between C29 and C46 of a single HokB peptide and that this reduction is essential for persistence. To verify this, we performed a persistence assay following expression of $hokB_{Y29}$ which contains a non-editable tyrosine codon at position 29 (Fig. 4C) (Bar-Yaacov et al. 2017). In a wild-type background, $hokB_{Y29}$ expression still increases persistence, indicating that RNA editing does not affect HokB-mediated persistence. However, the presence of a non-editable tyrosine at position 29 abolishes the dominant negative effect of HokB expression in the Δ*dsbC* mutant. As DsbA preferentially forms a disulfide bridge between two consecutive cysteine residues (Depuydt, Messens, and Collet 2011), the dominant negative effect therefore likely

results from the absence of isomerization of HokB after RNA editing, resulting in cell death after 2 to 3 cell divisions (Fig. S4B). This is in line with a previous report showing that genetically substituting Y29 by a cysteine induces cell death (Bar-Yaacov et al. 2017).

The absence of high persister counts following *hokB* expression in Δ*dsbC* mutants can be explained either by an impaired induction of persistence or an impaired awakening of persister cells. As we previously discovered a link between pore functioning and persistence (Wilmaerts et al. 2018), we hypothesized that in the case of impaired induction of persistence, HokB pores would not be functional. Therefore, different characteristics of HokB pore functioning, i.e. membrane depolarization and ATP leakage (Wilmaerts et al. 2018; Verstraeten et al. 2015), were assessed in the Δ*dsbC* mutant. $HokB_{Y29}$ was used instead of HokB in the Δ*dsbC* mutant to avoid incorrect ATP measurements resulting from cell lysis. As is the case in the wild type, expression of $hokB_{Y29}$ in a Δ*dsbC* mutant still evokes membrane depolarization (Fig. 4D), and ATP leakage (Fig. 4E), indicating that HokB still forms functional pores in the absence of DsbC. These findings suggest that all mechanisms are in place to induce persistence and that the low persister level upon *hokB* expression in a Δ*dsbC* strain is due to an impaired awakening of persister cells.

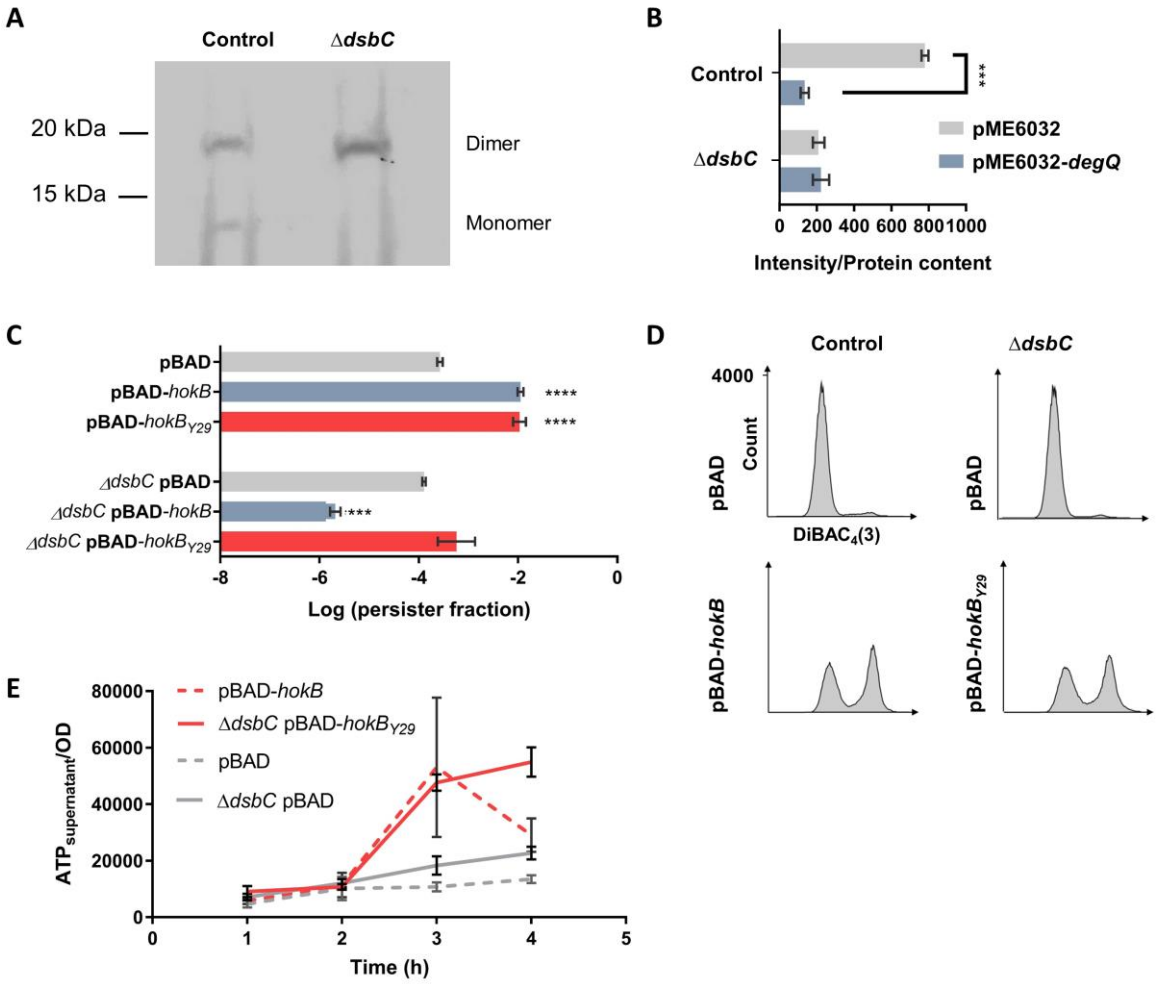


**Figure 4. HokB pores are functional in a Δ*dsbC* mutant.** (A) In the absence of DsbC, 100% of HokB peptides are in the dimer form. A representative example of three independent experiments is shown. (B) A reducing western blot was performed to assess the HokB peptide concentration. Signal intensities from the band were divided by the total protein concentration of the sample. DegQ-mediated degradation of HokB is constrained in a Δ*dsbC* mutant. HokB peptide levels upon *degQ* expression are diminished significantly in the wild-type background, in contrast to the Δ*dsbC* mutant. Values are means ± SEM from at least three independent experiments. Asterisks indicate statistically significant differences from the vector control (*** $P < 0.0001$). Data for the wild-type background are identical to the data shown in Fig. 3A. (C) Expression of *hokB* in a Δ*dsbC* mutant causes a dominant negative

effect which results from RNA editing, as expression of *hokB*$_{Y29}$ does not cause this phenotype. Expression of *hokB*$_{Y29}$ in the wild type does not affect persistence. Values are means ± SEM from at least three independent experiments. Asterisks indicate statistically significant differences from the empty vector control (**** $P < 0.0001$). See also Figure S4A and S4B. (D) Expression of *hokB* depolarizes the membrane in the wild-type background and in a Δ*dsbC* mutant. A representative example of at least 3 independent repeats is shown. (E) HokB pores result in ATP leakage after 3 h induction in both the wild type and the Δ*dsbC* mutant. Values are means ± SEM from at least three independent experiments. $P < 0.001$ for the comparison of Δ*dsbC* pBAD and pBAD-*hokB*$_{Y29}$ after 3 h and 4 h induction. $P < 0.05$ for the comparison of pBAD and pBAD-*hokB* in the wild-type background.

## Absence of the complex I component NuoA impairs persister awakening

Reduction of the disulfide bridge between HokB peptides renders these peptides vulnerable to DegQ-mediated degradation, resulting in pore disassembly. We have previously shown that HokB induces membrane depolarization and ATP leakage (Wilmaerts et al. 2018). Therefore, we hypothesized that in addition to pore disassembly, persister awakening also requires repolarization of the membrane to replenish cellular ATP levels.

To assess whether repolarization of the membrane is required for persister awakening, we used a mutant deprived of *nuoA.* NuoA is part of the NADH-dehydrogenase complex I (NDH-I), which consists of 13 subunits encoded by the *nuo* operon. Deletion of one gene in the operon abolishes complex I activity (Erhardt et al. 2012). NDH-I translocates two protons to the periplasm per transported electron, and as a consequence, disruption affects the cell's ability to repolarize the membrane. As expected, the effect of *hokB* expression on persistence is severely reduced in a Δ*nuoA* mutant (Fig. 5A). HokB pores are functional in the Δ*nuoA* mutant, as there is still membrane depolarization and ATP leakage (Fig. 5B, Fig. 5C). These data are similar to

the results obtained for the Δ*dsbC* mutant and indicate that persister awakening is impaired in the absence of NuoA.

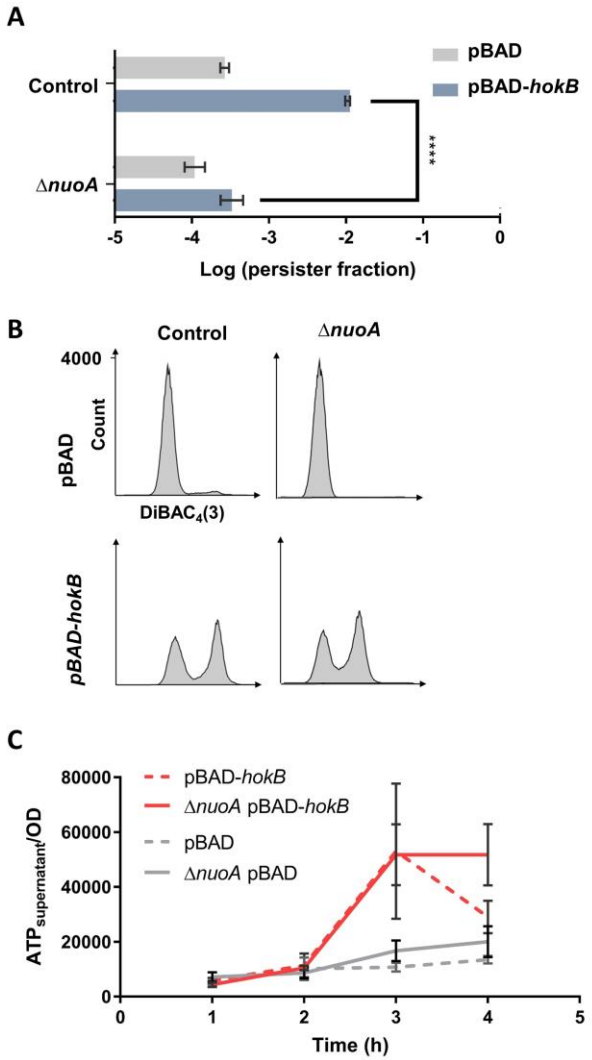


**Figure 5. HokB pores are functional in a Δ*nuoA* mutant.** (A) HokB-mediated persistence is strongly impaired in a Δ*nuoA* mutant. Values are means ± SEM from at least three independent experiments. Asterisks indicate statistically significant differences (**** $P < 0.0001$). (B) Membrane depolarization upon *hokB* expression was assessed using $DiBAC_4(3)$, showing that HokB still collapses the membrane potential in the Δ*nuoA* mutant. A representative example of three independent experiments is shown. (C) HokB pores result in ATP leakage after 3 h induction in both the wild type

and the Δ*nuoA* mutant. Values are means ± SEM from at least three independent experiments. After 3 h induction, $P < 0.05$ for the comparison of pBAD and pBAD-*hokB* in both backgrounds.

## Awakening of HokB-induced persisters relies on peptide monomerization and membrane repolarization

The preceding experiments demonstrate that HokB pores are functional in the Δ*dsbC* and Δ*nuoA* mutants (Fig. 4D, Fig. 4E, Fig. 5B, Fig. 5C), even though persister counts are not increased in these mutants following *hokB* expression (Fig. 4C, Fig. 5A). This suggests that awakening of HokB-induced persisters is impeded. To validate this hypothesis, the lag phase of individual persisters was assessed in various deletion mutants. In a wild-type background, HokB-induced persisters have a shortened lag phase compared to the empty vector control (Wilmaerts et al. 2018). However, expression of $hokB_{Y29}$ in Δ*dsbC* and *hokB* in Δ*nuoA* mutants delays awakening (Fig. 6A), indicating that regrowth is impaired. To confirm that DsbC-mediated monomerization is important for awakening, we assessed the lag phase following *hokB* expression in a Δ*trxA* mutant that has an impaired electron transport towards DsbC (Depuydt, Messens, and Collet 2011). The abolishment of DsbC's reducing capacity delays regrowth of HokB-induced persister cells (Fig. 6A), corroborating the importance of disulfide bridge reduction for awakening. Deletion of *degQ* does not affect the lag phase of HokB-induced persister cells, indicating that disassembly of HokB pores but not degradation of the constituting peptides drives persister awakening (Fig. 6A).

Our data show that the absence of DsbC and NuoA delays HokB-induced persister cell awakening (Fig. 6A). However, this does not explain the decreased persister fraction in these mutants compared to the wild type expressing *hokB* (Fig. 4C, Fig. 5A). Indeed, when quantifying persisters by plate counting, a mere delay of awakening would eventually yield

similar persister counts. Therefore, we hypothesized that absence of HokB monomerization or membrane repolarization restrains the growth resumption of HokB-induced persister cells and, hence, colony formation. To demonstrate that the population has more viable cells than assessed through plate counting, 10 000 metabolically active cells were sorted and the number of colonies on plate was counted. Data presented in Fig. 6B show that the fraction of regrowing cells is significantly higher in the wild-type control compared to the Δ*dsbC* and Δ*nuoA* mutants. This demonstrates that HokB-induced persister cells display reduced awakening in the absence of DsbC-mediated monomerization or complex-I-mediated membrane repolarization.

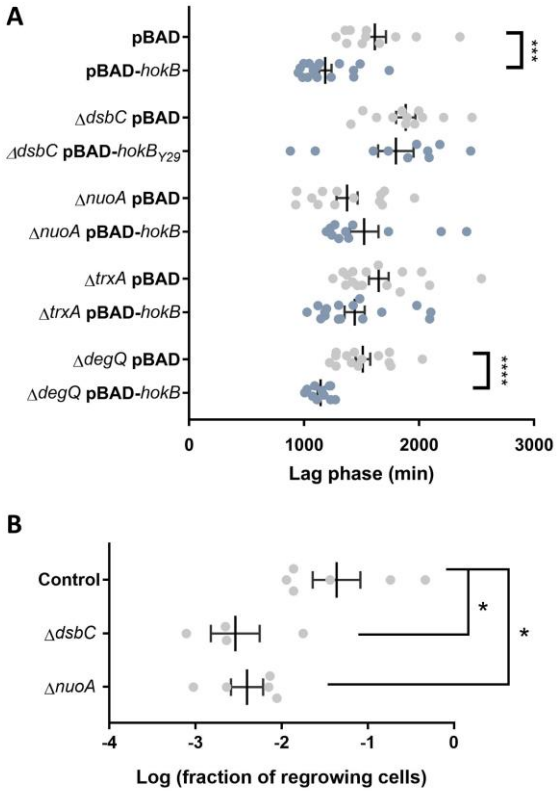


**Figure 6. Awakening of HokB-induced persister cells is hindered in absence of monomerization and membrane repolarization.** (A) HokB-induced persister cells have a shortened lag phase in the wild type and in the Δ*degQ* mutant. This reduction in lag phase is not observed when expressing *hokB*$_{Y29}$ in Δ*dsbC* and *hokB* in Δ*trxA* and Δ*nuoA* mutants. Values are means

± SEM from at least three independent experiments. Asterisks indicate statistically significant differences from the empty vector control (**** $P < 0.0001$; *** $P < 0.001$). (B) Stationary-phase cultures expressing *hokB* (*hokB*$_{Y29}$ in the case of the Δ*dsbC* mutant) were treated with antibiotics and stained with redox sensor green (RSG). The latter emits green fluorescence when cells are metabolically active and therefore acts as a measure for reducing capacity. For each sample, 10 000 highly fluorescent cells were sorted and plated. The number of colonies after antibiotic treatment was divided by the number of colonies of the control sample, after which the log was taken. Data from at least three independent experiments are represented and indicate the fraction of viable cells that are able to grow in the population after antibiotic treatment. Asterisks indicate statistically significant differences from the empty vector control (* $P < 0.05$).

## DISCUSSION

Several toxins have been implicated in persistence, but a detailed mode of action remains in many cases unknown (Korch and Hill 2006; Tripathi et al. 2014; Dörr, Vulić, and Lewis 2010). In previous work, we have shown that the conserved GTPase ObgE induces *hokB*, a type I toxin that is widespread amongst Gram-negative bacteria (Verstraeten et al. 2015). Furthermore, we have demonstrated that HokB forms pores that result in ATP leakage, which is linked with the induction of persistence (Wilmaerts et al. 2018). In the current study, we have identified several factors affecting HokB peptide stability and we have demonstrated that this stability plays a crucial role in both the induction of persistence and in the awakening process of HokB-induced persister cells.

### DsbA-mediated dimerization of HokB is required to induce persistence

In a wild-type background, the majority of the HokB peptides is detected in its dimeric form, with a relative monomer fraction of approximately 20%. Our results support a model in which dimerization is effectuated by the periplasmic oxidoreductase DsbA and results in an

intermolecular disulfide bridge between two periplasmic cysteine residues at position C46. The lower concentration of $HokB_{C46S}$ and the observation that HokB cannot be detected in a Δ*dsbA* mutant demonstrate that HokB monomers are unstable. This accords with earlier observations, demonstrating that disulfide bridge formation stabilizes a peptide (Denoncin and Collet 2013). In addition, expression of $HokB_{C46S}$ does not increase persister levels, indicating that dimerization is required for the induction of persistence. Noteworthy, a tyrosine-to-cysteine change at position 29 mediated by RNA editing presumably results in DsbA preferentially forming an intramolecular disulfide bridge between the two consecutive C29 and C46 residues (Depuydt, Messens, and Collet 2011). This intramolecular bridge was shown to be deleterious to the cell (Bar-Yaacov et al. 2017), and our data are indicative of a rescue mechanism that is mediated by the disulfide oxidoreductase DsbC.

### HokB peptide destabilization and membrane repolarization modulate persister awakening

Tracking regrowth via microfluidics and single-cell sorting revealed a positive correlation between the dormancy duration of HokB-induced persister cells and the concentration of HokB peptides. This is in line with previous research conducted using an exponentially-growing *E. coli* population, for which it was shown that the duration of growth arrest depends on the concentration of the HipA toxin (Rotem et al. 2010). Intriguingly, regrowing HokB-induced persister cells have aberrant outgrowth phenotypes, which likely results from the antibiotic treatment. This demonstrates that the antibiotic target in persister cells is active, confirming an earlier report on persister cells acquiring DNA damage following antibiotic treatment (Völzing and Brynildsen 2015).

The normal distribution of the time to first cell division of HokB-induced persister cells indicates that one or multiple intermediate steps activate the awakening process (Norman et al. 2015). In addition, the positive correlation between the concentration of HokB peptides and the dormancy duration in persister cells suggests that molecular mechanisms initialize awakening by destabilizing HokB peptides, eventually resulting in pore disassembly. We found that HokB peptide destabilization is controlled by the oxidoreductase DsbC. In the absence of DsbC, HokB peptides are exclusively in the dimer configuration and form functional pores, as there is membrane depolarization and ATP leakage. However, expression of *hokB* in a Δ*dsbC* mutant does not increase persister counts, suggesting that awakening is impaired in this mutant. Corroborating this finding, the fraction of cells that are metabolically active but unable to grow is higher in a Δ*dsbC* mutant compared to the wild type. Some persisters do wake up, however, at a rate comparable to the empty vector control. The origin of these persisters can either be HokB-independent or -dependent. In the latter case, the disulfide bridge might be reduced by other reducing compounds in the periplasm, such as glutathione (Ke and Berkmen 2014).

HokB-induced persister cells display ATP leakage and membrane depolarization (Wilmaerts et al. 2018; Verstraeten et al. 2015). We reasoned that in order to resume growth, DsbC-mediated pore disassembly should be followed by replenishment of cellular energy pools and repolarization of the membrane. We found that membrane repolarization by complex I of the ETC plays a major role in HokB-persister cell awakening, although the role of other units of the ETC cannot be excluded. Absence of complex I leaves HokB pore characteristics unaltered. However, the number of metabolically active cells that are unable to grow is increased in a mutant deprived of complex I and, in addition, regrowth of persister cells is delayed. In conclusion, peptide destabilization by DsbC-mediated monomerization as well as repolarizing the membrane are essential for awakening of HokB-induced persister cells.

## DegQ degrades HokB monomers

Following monomerization by DsbC, HokB peptides need to be degraded to prevent re-dimerization and thus re-formation of the pore. Our results show that HokB peptide levels are controlled by the periplasmic DegQ protease. To the best of our knowledge, this is the first report of a protease targeting a type I toxin. DegQ is known to cleave next to an isoleucine or a valine residue (Kolmar, Waller, and Sauer 1996), the latter of which is present in the periplasmic amino acid sequence of HokB at position 40. Cleaving off the V40 residue would remove the C46 residue, thereby preventing re-dimerization of HokB peptides by DsbA. Noteworthy, DegQ shows highest activity at a relatively low pH of 5.5 *in vitro* (Sawa et al. 2011). The average periplasmic pH of *E. coli* is 7.5 (Wilks and Slonczewski 2007) and although it is unlikely that membrane repolarization would result in a periplasmic pH of 5.5, a small decrease due to proton translocation might modulate awakening of HokB-induced persister cells by triggering DegQ-mediated degradation.

Although deletion of *degQ* affects HokB-induced persistence to a certain extent, awakening of HokB-induced persister cells is not delayed in a Δ*degQ* mutant. This is in contrast to our results with Δ*dsbC* and Δ*nuoA* mutants and it might indicate that peptide destabilization and repolarization are the primary factors modulating awakening, or that the delayed lag phase in Δ*dsbC* and Δ*nuoA* mutants is HokB-independent. Alternatively, other proteases might take over upon *degQ* deletion, which is plausible given their redundant character (Sklar et al. 2007).

## A model for induction and awakening of HokB-induced persister cells

Taken together, we propose a model that explains both the induction and awakening of HokB-induced persister cells (Fig. 7). Following HokB peptide insertion into the membrane, the periplasmic oxidoreductase DsbA forms an intermolecular disulfide bridge, thereby stabilizing

HokB peptides and allowing pore formation. The latter causes ATP leakage and membrane depolarization, ultimately inducing persistence. Upon awakening, the oxidoreductase DsbC reduces the disulfide bridge, which disassembles the pore and allows the ETC to repolarize the membrane and produce ATP. Repolarization lowers the pH, which in turn activates DegQ to cleave off a part of the periplasmic domain of HokB monomers, thereby preventing re-dimerization. This ultimately results in the regrowth of HokB-induced persister cells.

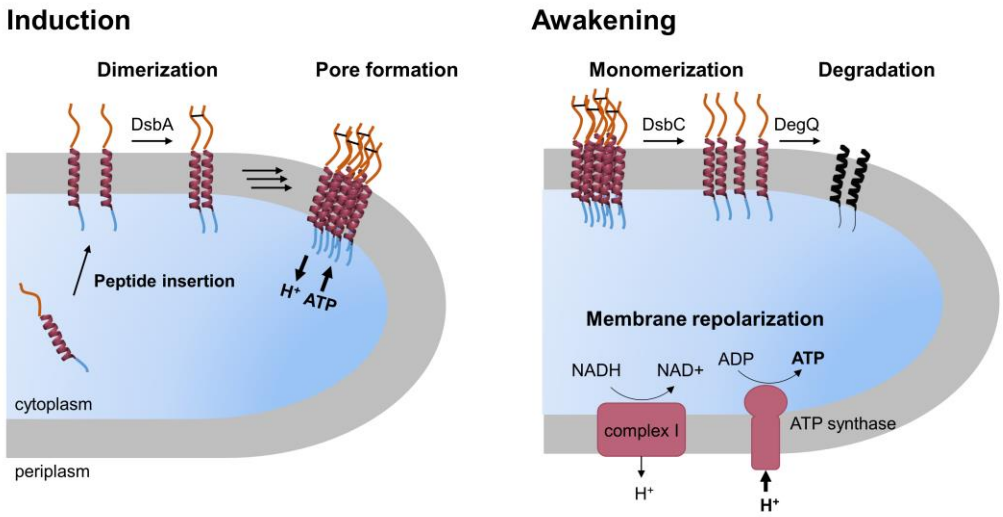


**Figure 7. Model of HokB-mediated persister induction and awakening.** Upon HokB peptide insertion in the membrane, DsbA catalyzes the formation of a disulfide bridge between the C46 residues of two HokB monomers. This stabilizes HokB peptides, allowing pore formation. Pore formation results in the leakage of protons and ATP out of the cell, inducing persistence. HokB pores are destabilized via DsbC-mediated monomerization. This targets HokB peptides for degradation by DegQ. Once the pore is dysfunctional, the electron transport chain is able to repolarize the membrane and replenish the ATP pool, eventually resulting in persister cell awakening. Of note, an intramolecular bridge between a C29 residue and the C46 residue can be formed after adenosine-to-inosine RNA editing of tyrosine 29. However, this is bridge is not implicated in the persister phenotype.

## ACKNOWLEDGEMENTS

This work was supported by grants from the FWO (G055517N, G047112N, G0B2515N) and the Interuniversity Attraction Poles-Belgian Science Policy Office IAP-BELSPO (IAP P7/28). We thank Serge Beullens for the technical assistance with FACS and David De Coster for his assistance with western blotting.

## AUTHOR CONTRIBUTIONS

D.W. designed and performed the experiments, analyzed the data and wrote the manuscript. L.D., N.V. and J.M. designed the experiments, discussed the results and edited the manuscript. P.J.D.L. and C.B. helped in performing the experiments.

## DECLARATION OF INTEREST

The authors declare no competing interests.

## STAR METHODS

### Contact for reagent and resource sharing

Further information and requests for recourses and reagents should be directed to and will be fulfilled by the Lead Contact, Jan Michiels (jan.michiels@kuleuven.vib.be).

### Experimental model and subject details

*E. coli* TOP10, obtained from Invitrogen (USA), was used in all experiments. Bacteria were grown in autoclaved lysogeny broth (LB) at 37°C. Liquid cultures were incubated with orbital shaking (200 rpm) in the presence of appropriate antibiotics. Strains containing the pBAD/His A plasmid were cultured in LB with 100 µg $ml^{-1}$ ampicillin. Strains containing the pME6032 plasmid were cultured in LB with 10 µg $ml^{-1}$ tetracycline.

## Method details

### Bacterial strain construction

The Δ*dsbA*, Δ*dsbC,* Δ*nuoA,* Δ*degQ* and Δ*trxA* knockout mutants were made by homologous recombination following the protocol of Datsenko & Wanner (Datsenko and Wanner 2000). The following primers were used: AGAACCCCCTTTGCAATTAA and GCAACAATAACACCTGTAGC (Δ*dsbA*), ATCACCGACCACAATAATCC and GTTTACTGGCTGGAAACCTA (Δ*dsbC*), ACGTTCTTTGCCGATAGATT and GCAGAACGTACAAAACTGTT (Δ*nuoA*), TACCATGGCGCACGACTATC and CTGCATCATGACCGCTAGCC (Δ*degQ*) and AGGGCGAAGTCGGAAAACTT and CATGTCTTTTCGCTGCCTGG (Δ*trxA*).

For the construction of pBAD/His A-$hokB_{C9S,}$ pBAD/His A-$hokB_{C14S}$ and pBAD/His A-$hokB_{C46S,}$ gene blocks (Table 1) were ordered from IDT (USA) and cloned in pBAD/His A using KpnI and HindIII restriction. The mutated *hokB* fragments were amplified by PCR using primers CACCGGTACCGGATCAGGTTCCGGCTCTAAGCACAACCCTCTGG and ATCGAAGCTTTTACCTGGACGTGCA. The PCR products were digested with KpnI and HindIII and cloned into pBAD/*Myc*-His A-*mCherry* (Shaner et al. 2004). Similarly, pBAD/His A-$hokB_{Y29}$ was constructed by amplifying the mutated *hokB*-fragment from pBAD/*Myc*-His A-*mCherry*-$hokB_{Y29}$ (Bar-Yaacov et al. 2017) and transferring the resulting product to pBAD/His A. The protease-encoding genes *degQ*, *mepA*, *hslU*, *elaD*, *rseP*, *degP*, *ptrA*, *prc*, *ftsH* and *hslV* were expressed using plasmids from the ASKA library (Kitagawa et al. 2005). pME6032-*degQ* was constructed by amplifying *degQ* from *E. coli* BW25113 using primers CACCGGTACCATGAAAAAACAAACC and ACTGCTCGAGTTAACGATCAGCAG. The PCR product was digested using KpnI and XhoI and cloned into PME6032. Construction of pBAD/*Myc*-His A-*perceval,* pBAD/His A-*hokB* and pBAD/*Myc*-His A-*mCherry-hokB* was described previously (Verstraeten et al. 2015; Wilmaerts et al. 2018).

620 **Table 1** DNA sequences of HokB substitution mutants.

| | |
|---|---|
| *hokB*$_{C9S}$ | CACCCTCGAGATGAAGCACAACCCTCTGGTGGTGTCCCTGCTCATTATCTGCATTACGATT CTGACATTCACACTCCTGACCCGACAAACGCTCTACGAACTGCGGTTCCGGGACGGTGAT AAGGAGGTTGCTGCGCTCATGGCCTGCACGTCCAGGTAAGGGCAAGCGCGGGGATTTTC CCCGCGCATTTGACTAGCAGATTCATTTTCTCATGGCACCCCTTTTACACTTCAGTTAGTG CATGTTTTTTTCGATGCACTAATAGAACCATCATTACAGACAAATTTGCCGCCTGCCGTAC AGTGTGAGATCCCAAGCTTGATC |
| *hokB*$_{C14S}$ | CACCCTCGAGATGAAGCACAACCCTCTGGTGGTGTGTCTGCTCATTATCTCCATTACGATT CTGACATTCACACTCCTGACCCGACAAACGCTCTACGAACTGCGGTTCCGGGACGGTGAT AAGGAGGTTGCTGCGCTCATGGCCTGCACGTCCAGGTAAGGGCAAGCGCGGGGATTTTC CCCGCGCATTTGACTAGCAGATTCATTTTCTCATGGCACCCCTTTTACACTTCAGTTAGTG CATGTTTTTTTCGATGCACTAATAGAACCATCATTACAGACAAATTTGCCGCCTGCCGTAC AGTGTGAGATCCCAAGCTTGATC |
| *hokB*$_{C46S}$ | CACCCTCGAGATGAAGCACAACCCTCTGGTGGTGTGTCTGCTCATTATCTGCATTACGATT CTGACATTCACACTCCTGACCCGACAAACGCTCTACGAACTGCGGTTCCGGGACGGTGAT AAGGAGGTTGCTGCGCTCATGGCCTCCACGTCCAGGTAAGGGCAAGCGCGGGGATTTTC CCCGCGCATTTGACTAGCAGATTCATTTTCTCATGGCACCCCTTTTACACTTCAGTTAGTG CATGTTTTTTTCGATGCACTAATAGAACCATCATTACAGACAAATTTGCCGCCTGCCGTAC AGTGTGAGATCCCAAGCTTGATC |

621

622 Persistence assay

623 Persistence assays were performed in stationary phase. Overnight cultures were diluted 100-
624 fold in 250 mL flasks containing 100 ml LB medium, appropriate antibiotics (ampicillin (100
625 μg mL$^{-1}$) and/or tetracycline (10 μg mL$^{-1}$)) and inducer (0.2% arabinose and/or IPTG (1mM)).
626 For experiments shown in Fig. S1C and Fig. S4A, DTT was prepared freshly, filter sterilized
627 and added at a concentration of 10 μM or 3 mM to the LB medium after autoclaving. Cultures

were incubated for 16-18 h, after which 990 µL was treated with 5 µg $mL^{-1}$ ofloxacin (10 µL sterile water was added to the control). After 5 h incubation, samples were serially diluted in 10 mM $MgSO_4$, plated on LB-agar plates and incubated for 48 h at 37°C. The number of colony forming units (CFUs) was determined by plate counting.

### Purification of the membrane fraction and western blot

Overnight cultures were diluted 100-fold and induced in test tubes with 5 mL LB, and appropriate inducers and antibiotics were added. After 16 h incubation, 2 mL of culture was spun down (13000 rpm, 5 min) and frozen overnight at -20°. Samples were dissolved in 300 µL EDTA-free protease inhibitor, 100 mM iodoacetamide (IAM) and benzonase (all purchased from Sigma Aldrich). Samples were sonicated for 2 min at 15% amplitude with a Branson digital sonifier, after which they were centrifuged for 70 min at 15000 rpm at 4°C. After centrifugation, the supernatant was removed and the pellet was dissolved in 8 M urea (purchased from VWR International) and 100 mM IAM. Samples were dissolved in NuPAGE LDS Sample buffer (Invitrogen) (for a reducing western blot in combination with NuPAGE LDS Reducing agent (Invitrogen)), and incubated for 20 min at 70°C, after which they were loaded on a Novex ® 12% Tris-Glycine Gel (Invitrogen) in MES-buffer in a Novex Bolt Mini Gel tank.

Proteins were transferred using a XCell Sure Lock on a PVDF Membrane filter paper in CAPS buffer. The membrane was blocked for 1 h using bovine serum albumin (BSA) (1%) dissolved in TBS buffer, and subsequently washed with TBS in case anti-His6 (mouse IgG1) monoclonal antibodies (Sigma-Aldrich) were used at a concentration of 0.2 µg $mL^{-1}$, as recommended by the manufacturer. In case HisProbe™-HRP (Thermo Scientific™) antibodies were used, at a concentration of 1 µg $mL^{-1}$, the membrane was blocked for 2 h using skimmed milk and 0.1%

Tween20. After blocking, the membrane was incubated overnight at 4°C in shaking conditions. The membrane was washed using 0.1% Tween20 in TBS buffer. In case anti-His6 monoclonal antibodies were used, anti-Mouse IgG – Alkaline Phosphatase (Sigma Aldrich) antibodies were incubated for 1 h at room temperature at a concentration of 1.2 µg $mL^{-1}$, as recommended by the manufacturer, after which the blot was washed using 0.1% Tween20 in TBS buffer. Following the color reaction, a picture was taken from the blot using a Canon EOS 1300D camera, after which the picture was reverted to grayscale using GIMP software. Using the HisProbe™-HRP, detection occurred immediately after washing using the Clarity™ Western ECL Substrate (Bio-Rad) and the Fusion FX imaging system (Vilber Lourmat).

Pictures were uploaded to Image Studio Lite®, after which signal intensities from the bands could be detected. For quantitative assays of protein concentration between different strains, corrections of the signal intensities were made based on the total protein concentration of the sample, measured using the Qubit™ protein assay kit (Invitrogen™).

### Measuring the membrane potential

The membrane potential was measured as described before (Wilmaerts et al. 2018). Briefly, strains incubated overnight were diluted 100-fold in PBS buffer containing $DIBAC_4(3)$ (Invitrogen™).

### Measuring ATP in the supernatant

The concentration of ATP in the supernatant was measured as described before (Wilmaerts et al. 2018). Briefly, strains incubated overnight were diluted 100-fold in 100 mL LB medium, after which the cells were kept on ice for 5 min and centrifuged for 10 min at 5000 rpm. 100 µL BacTiter-Glo reagent (Promega, USA) was added to 100 µL of the supernatant. After 5 min

incubation at room temperature, bioluminescence and OD (595 nm) measurements were taken for every well. The bioluminescence was divided over the OD.

### Measuring the time to first cell division using microfluidics

An overnight culture was diluted 100 times in 5 mL LB. For exponential-phase cultures, bacteria were incubated for 3 h at 37°C, after which they were treated with ceftazidime (500 μg $mL^{-1}$) for 4 h. For stationary-phase cultures, samples were incubated for 16h at 37°C, after which they were treated with ofloxacin (5 μg $mL^{-1}$) for 5 h. Following antibiotic treatment, cells were spun down at low speed (3000 rpm, 5 min) and dissolved in LB medium that was preheated to 37°C. The microfluidic device was prepared following the manufacturer's instructions. After cell loading, fluorescence images were taken immediately using a Nikon Eclipse Ti-E inverted microscope with a CFI Plan Apochromat 100X objective with a numerical aperture of 1.45. Fluorescence intensity of the cells was analyzed using the NIS Elements Analysis 4.4 software (Nikon, Japan). LB was added to the chamber with a pressure of 1.2 psi for 24 h at 37°C. Phase-contrast images were taken every 15 min for 24 h. For exponential-phase persisters, differences in fluorescence intensity of the population between different days were taken into account by calculating the average fluorescence intensity of the surviving cells (not lysed) and dividing it by the fluorescence intensity of the regrowing persister cells. For stationary-phase cells, all persisters originated from a single experiment.

### Measuring single-cell lag time

Single-cell lag times were measured as described before (Wilmaerts et al. 2018). Briefly, cells were incubated an treated with antibiotics as described for the persistence assay. After ofloxacin treatment (5 μg $mL^{-1}$), cells were resuspended in LB, after which a twofold dilution series was prepared. A growth curve was obtained by incubating cells in a Bioscreen C device

under continuous shaking at 37°C. If two consecutive wells displayed no growth, the well before was assigned to contain a single cell (Francois et al. 2003). Single-cell lag times were calculated using the Gompertz equation (Zwietering et al. 1990).

### Measuring the lag time after fluorescence activated cell sorting

Antibiotic treatment was performed as described for the microfluidics assay. Subsequently, samples were dissolved in PBS buffer (pH = 7.4) at room temperature and individual cells were immediately collected in a honeycomb plate. During sorting, the fluorescence intensity of each cell was linked with its position. Sorting was gated on the forward and side scatter of a non-treated population. After sorting, the plates were incubated in a Bioscreen C device under continuous shaking at 37°C for 48 h and the OD at 595 nm was measured every 15 min. The lag phase of each persister cell was calculated from the growth curve using the Gompertz equation (Zwietering et al. 1990). To take into account differences in fluorescence intensity of the population between different days, the average fluorescence intensity of the surviving cells was calculated and divided by the fluorescence intensity of the resuscitated persister cells.

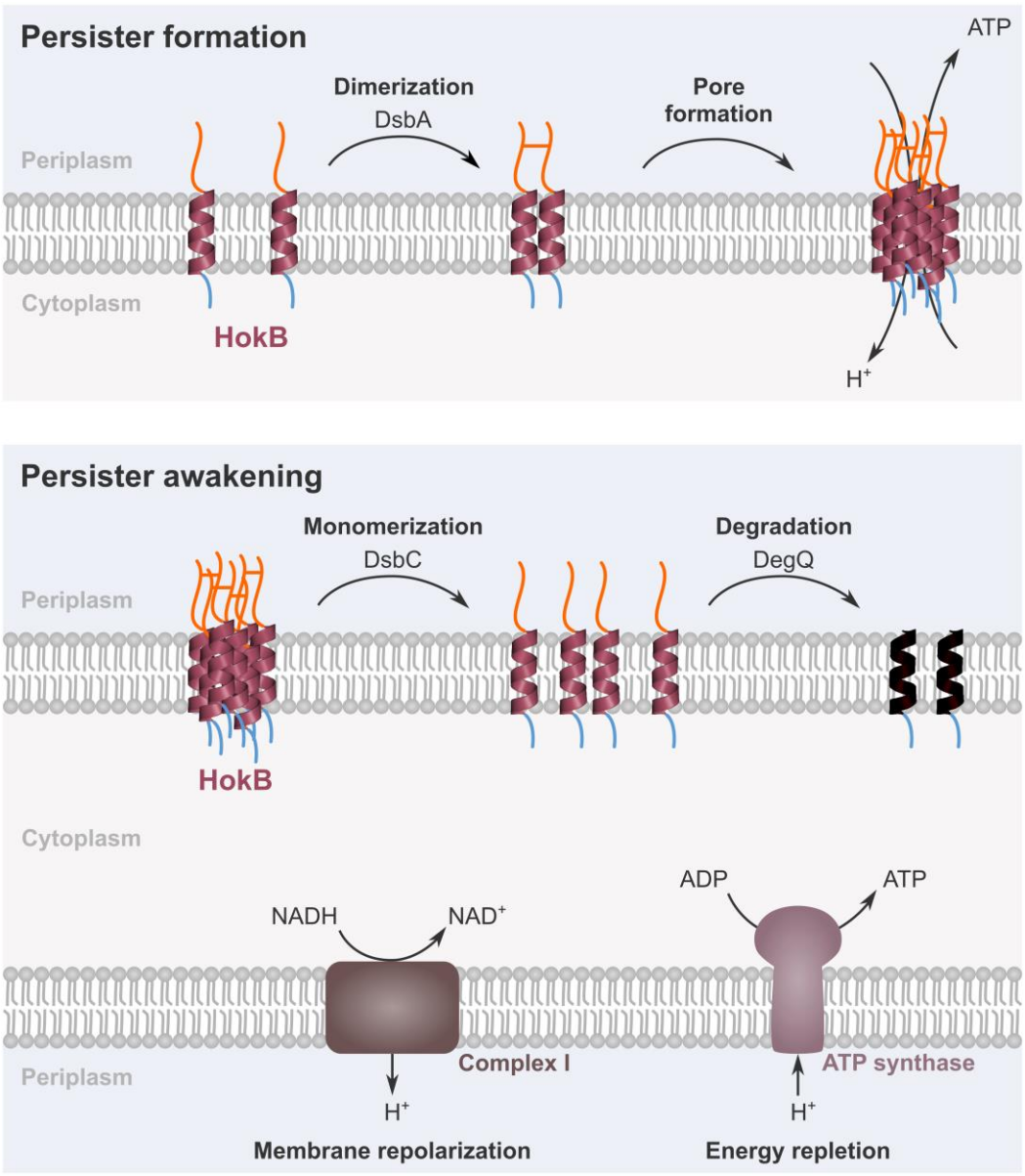


717

718 Assessing viable cells in the population

719 A persister assay in stationary phase was performed as described above. Antibiotic-treated cells
720 were centrifuged (3000 rpm, 5 min) and dissolved in 1 mL PBS in combination with redox
721 sensor green (RSG), purchased from Invitrogen (USA). For the control samples, 20 µL of the
722 untreated culture was taken and dissolved in 1 mL PBS with RSG. After 10 min incubation at
723 room temperature, cells were sorted based on a high RSG value, which was determined using
724 exponentially-growing cells that had grown for 3 h after 100-fold dilution in 5 mL LB. After
725 determining the appropriate gate, 10 000 cells were sorted in 1 mL PBS for both conditions.

After sorting, the antibiotic-treated samples were centrifuged (3000 rpm, 5 min) and diluted in 110 µL 10 mM $MgSO_4$, after which they were plated on LB agar plates. The control samples were directly diluted in 10 mM $MgSO_4$, after which they were plated on LB agar plates. Plates were incubated for 48 h at 37°C and the number of CFUs was quantified by plate counting. To determine the fraction of cells that, after antibiotic treatment, was able to regrow in the whole population of viable cells, the number of CFUs per mL of the antibiotic-treated sample was divided by the number of CFUs per mL of the control sample. Cells were sorted using a BD influx cell sorter (BD Biosciences, USA) and RSG fluorescence was measured using a 488-nm laser and a 520-nm filter. Data were analyzed using FlowJo V10 (BD Biosciences, USA).

## Quantification and statistical analysis

### Persistence assay

Statistical calculations were performed on log10-transformed data and were used to verify potential differences in persister fractions. Statistical comparisons were based on ANOVA with a Tukey's post hoc test for multiple comparisons for more than two populations, and an unpaired two-sided t-test was used to compare the means of two populations.

### Measuring ATP leakage, single-cell lag times and determining viable cells

Statistical comparisons were made using an unpaired two-sided t-test.

### Determination of relative monomer fraction and total protein concentration

Statistical comparisons for the relative monomer fractions for the substitution mutants were based on ANOVA with a Dunnett's post hoc test for multiple comparisons. To determine a statistical difference between total protein concentrations, corrected by the total protein concentration, unpaired two-sided t-test were used to compare the means of two populations.

Differences in signal intensity over the total protein content are explained by the presence of the pME6032 plasmid (Fig. 3A). Additionally, the differences in signal intensities over the total protein content between the HokB controls in Fig 1C and Fig. 3E result from using different detection methods. For Fig. 1C, HisProbe-HRP antibodies were used, while for Fig. 3E, anti-His6 monoclonal antibodies were used.

### Correlation analysis

Spearman correlation was used to determine the correlation between time to first cell division and fluorescence intensity.

### Determination of statistical difference between flow cytometric data

Statistical differences between flow cytometric data were assessed using the Chi squared comparison algorithm of the FlowJo software. The obtained T(x) values between *hokB* expressed in the wild-type background and the Δ*degQ* mutant were not statistically different from the controls.

## REFERENCES

Balaban, Nathalie Q., Jack Merrin, Remy Chait, Lukasz Kowalik, and Stanislas Leibler. 2004. “Bacterial Persistence as a Phenotypic Switch.” *Science* 305 (5690):1622–25. https://doi.org/10.1126/science.1099390.

Bar-Yaacov, Dan, Ernest Mordret, Ruth Towers, Tammy Biniashvili, Clara Soyris, Schraga Schwartz, Orna Dahan, and Yitzhak Pilpel. 2017. “RNA Editing in Bacteria Recodes Multiple Proteins and Regulates an Evolutionarily Conserved Toxin-Antitoxin System.” *Genome Research* 27 (10):1696–1703. https://doi.org/10.1101/gr.222760.117.

Bardwell, J C, K McGovern, and J Beckwith. 1991. “Identification of a Protein Required for

776 Disulfide Bond Formation in Vivo.” *Cell* 67 (3):581–89. https://doi.org/0092-
777 8674(91)90532-4 [pii].
778 Buerger, S., A. Spoering, E. Gavrish, C. Leslin, L. Ling, and S. S. Epstein. 2012. “Microbial
779 Scout Hypothesis, Stochastic Exit from Dormancy, and the Nature of Slow Growers.”
780 *Applied and Environmental Microbiology* 78 (9):3221–28.
781 https://doi.org/10.1128/AEM.07307-11.
782 Cheverton, Angela M., Bridget Gollan, Michal Przydacz, Chi T. Wong, Anastasia Mylona,
783 Stephen A. Hare, and Sophie Helaine. 2016. “A *Salmonella* Toxin Promotes Persister
784 Formation through Acetylation of TRNA.” *Molecular Cell* 63 (1):86–96.
785 https://doi.org/10.1016/j.molcel.2016.05.002.
786 Datsenko, K. A., and B. L. Wanner. 2000. “One-Step Inactivation of Chromosomal Genes in
787 *Escherichia coli* K-12 Using PCR Products.” *Proc Natl Acad Sci U S A* 97 (12):6640–
788 45. https://doi.org/10.1073/pnas.120163297.
789 Denoncin, Katleen, and Jean-François Collet. 2013. “Disulfide Bond Formation in the
790 Bacterial Periplasm: Major Achievements and Challenges Ahead.” *Antioxidants &*
791 *Redox Signaling* 19:63–71. https://doi.org/10.1089/ars.2012.4864.
792 Depuydt, Matthieu, Joris Messens, and Jean-Francois Collet. 2011. “How Proteins Form
793 Disulfide Bonds.” *Antioxidants & Redox Signaling* 15 (1):49–66.
794 https://doi.org/10.1089/ars.2010.3575.
795 Dörr, Tobias, Marin Vulić, and Kim Lewis. 2010. “Ciprofloxacin Causes Persister Formation
796 by Inducing the TisB Toxin in *Escherichia coli*.” *PLoS Biology* 8 (2):e1000317.
797 https://doi.org/10.1371/journal.pbio.1000317.
798 Dworkin, Jonathan, and Ishita M. Shah. 2010. “Exit from Dormancy in Microbial
799 Organisms.” *Nature Reviews Microbiology* 8 (12):890–96.
800 https://doi.org/10.1038/nrmicro2453.

Erhardt, Heiko, Stefan Steimle, Vera Muders, Thomas Pohl, Julia Walter, and Thorsten Friedrich. 2012. “Disruption of Individual Nuo-Genes Leads to the Formation of Partially Assembled NADH:Ubiquinone Oxidoreductase (Complex I) in *Escherichia coli*.” *Biochimica et Biophysica Acta - Bioenergetics* 1817 (6):863–71. https://doi.org/10.1016/j.bbabio.2011.10.008.

Francois, K., F. Devlieghere, A. R. Standaert, A. H. Geeraerd, J. F. Van Impe, and J. Debevere. 2003. “Modelling the Individual Cell Lag Phase. Isolating Single Cells: Protocol Development.” *Letters in Applied Microbiology* 37:26–30. https://doi.org/10.1046/j.1472-765X.2003.01340.x.

Gerdes, Kenn. 2016. “Hypothesis: Type I Toxin-Antitoxin Genes Enter the Persistence Field-a Feedback Mechanism Explaining Membrane Homoeostasis.” *Philosophical Transactions of the Royal Society of London. Series B, Biological Sciences* 371 (1707):20160189. https://doi.org/10.1098/rstb.2016.0189.

Goormaghtigh, Frédéric, Nathan Fraikin, Marta Putrinš, Thibaut Hallaert, Vasili Hauryliuk, Abel Garcia-Pino, Andreas Sjödin, et al. 2018. “Reassessing the Role of Type II Toxin-Antitoxin Systems in Formation of *Escherichia coli* Type II Persister Cells.” *mBio* 9 (3):e00640-18. https://doi.org/10.1128/mBio.00640-18.

Harms, Alexander, Ditlev Egeskov Brodersen, Namiko Mitarai, and Kenn Gerdes. 2018. “Toxins, Targets, and Triggers: An Overview of Toxin-Antitoxin Biology.” *Molecular Cell* 70 (5):768–84. https://doi.org/10.1016/j.molcel.2018.01.003.

Harms, Alexander, Cinzia Fino, Michael A. Sørensen, Szabolcs Semsey, and Kenn Gerdes. 2017. “Prophages and Growth Dynamics Confound Experimental Results with Antibiotic-Tolerant Persister Cells.” *mBio* 8 (6):e01964-17. https://doi.org/10.1128/mBio.01964-17.

Hayes, M V, and D C Orr. 1983. “Mode of Action of Ceftazidime: Affinity for the Penicillin-

826 Binding Proteins of *Escherichia coli* K12, *Pseudomonas Aeruginosa* and
827 *Staphylococcus Aureus*." *The Journal of Antimicrobial Chemotherapy* 12 (2):119–26.
828 Holden, David W., and Jeff Errington. 2018. "Type II Toxin-Antitoxin Systems and Persister
829 Cells." *mBio* 9 (5):e10574-18. https://doi.org/10.1128/mBio.01574-18.
830 Jõers, Arvi, Niilo Kaldalu, and Tanel Tenson. 2010. "The Frequency of Persisters in
831 *Escherichia coli* Reflects the Kinetics of Awakening from Dormancy." *Journal of*
832 *Bacteriology* 192 (13):3379–84. https://doi.org/10.1128/JB.00056-10.
833 Ke, Na, and Mehmet Berkmen. 2014. "Production of Disulfide-Bonded Proteins in
834 *Escherichia coli*." *Current Protocols in Molecular Biology* 82 (1):240–51.
835 https://doi.org/10.1002/0471142727.mb1601bs108.
836 Keren, Iris, Devang Shah, Amy Spoering, Niilo Kaldalu, and Kim Lewis. 2004. "Specialized
837 Persister Cells and the Mechanism of Multidrug Tolerance in *Escherichia coli*." *Journal*
838 *of Bacteriology* 186 (24):8172–80. https://doi.org/10.1128/JB.186.24.8172.
839 Kim, Jun-Seob, Ryota Yamasaki, Sooyeon Song, Weiwei Zhang, and Thomas K. Wood.
840 2018. "Single Cell Observations Show Persister Cells Wake Based on Ribosome
841 Content." *Environmental Microbiology* 20 (6):2085–98. https://doi.org/10.1111/1462-
842 2920.14093.
843 Kim, Younghoon, and Thomas K. Wood. 2010. "Toxins Hha and CspD and Small RNA
844 Regulator Hfq Are Involved in Persister Cell Formation through MqsR in *Escherichia*
845 *coli*." *Biochemical and Biophysical Research Communications* 391 (1):209–13.
846 https://doi.org/10.1016/j.bbrc.2009.11.033.
847 Kitagawa, Masanari, Takeshi Ara, Mohammad Arifuzzaman, Tomoko Ioka-Nakamichi, Eiji
848 Inamoto, Hiromi Toyonaga, and Hirotada Mori. 2005. "Complete Set of ORF Clones of
849 *Escherichia coli* ASKA Library (A Complete Set of *E. coli* K-12 ORF Archive): Unique
850 Resources for Biological Research." *DNA Research* 12 (5):291–99.

https://doi.org/10.1093/dnares/dsi012.

Kolmar, Harald, Patrick R.H. Waller, and Robert T. Sauer. 1996. “The DegP and DegQ Periplasmic Endoproteases of *Escherichia coli*: Specificity for Cleavage Sites and Substrate Conformation.” *Journal of Bacteriology* 178 (20):5925–29. https://doi.org/10.1128/jb.178.20.5925-5929.1996.

Korch, Shaleen B., and Thomas M. Hill. 2006. “Ectopic Overexpression of Wild-Type and Mutant *HipA* Genes in *Escherichia coli*: Effects on Macromolecular Synthesis and Persister Formation.” *Journal of Bacteriology* 188 (11):3826–36. https://doi.org/10.1128/JB.01740-05.

Michiels, Joran Elie, Bram Van den Bergh, Natalie Verstraeten, and Jan Michiels. 2016. “Molecular Mechanisms and Clinical Implications of Bacterial Persistence.” *Drug Resistance Updates* 29:76–89. https://doi.org/10.1016/j.drup.2016.10.002.

Mok, Wendy W K, and Mark P Brynildsen. 2018. “Timing of DNA Damage Responses Impacts Persistence to Fluoroquinolones.” *Proceedings of the National Academy of Sciences of the United States of America* 115 (27):e6301–9. https://doi.org/10.1073/pnas.1804218115.

Muthuramalingam, Meenakumari, John C. White, and Christina R. Bourne. 2016. “Toxin-Antitoxin Modules Are Pliable Switches Activated by Multiple Protease Pathways.” *Toxins* 8 (7):214–30. https://doi.org/10.3390/toxins8070214.

Norman, Thomas M., Nathan D. Lord, Johan Paulsson, and Richard Losick. 2015. “Stochastic Switching of Cell Fate in Microbes.” *Annual Review of Microbiology* 69:381–403. https://doi.org/10.1146/annurev-micro-091213-112852.

Orman, Mehmet A., and Mark P. Brynildsen. 2013. “Dormancy Is Not Necessary or Sufficient for Bacterial Persistence.” *Antimicrobial Agents and Chemotherapy* 57 (7):3230–39. https://doi.org/10.1128/AAC.00243-13.

876 Orman, Mehmet A., and Mark P. Brynildsen. 2015. “Inhibition of Stationary Phase
877 Respiration Impairs Persister Formation in *E. coli*.” *Nature Communications* 6 (7983).
878 https://doi.org/10.1038/ncomms8983.
879 Page, Rebecca, and Wolfgang Peti. 2016. “Toxin-Antitoxin Systems in Bacterial Growth
880 Arrest and Persistence.” *Nature Chemical Biology* 12 (4):208–14.
881 https://doi.org/10.1038/nchembio.2044.
882 Rotem, Eitan, Adiel Loinger, Irine Ronin, Irit Levin-Reisman, Chana Gabay, Noam Shoresh,
883 Ofer Biham, and Nathalie Q. Balaban. 2010. “Regulation of Phenotypic Variability by a
884 Threshold-Based Mechanism Underlies Bacterial Persistence.” *Proc Natl Acad Sci U S*
885 *A* 107 (28):12541–46. https://doi.org/10.1073/pnas.1004333107.
886 Sauvage, Eric, Frédéric Kerff, Mohammed Terrak, Juan A. Ayala, and Paulette Charlier.
887 2008. “The Penicillin-Binding Proteins: Structure and Role in Peptidoglycan
888 Biosynthesis.” *FEMS Microbiology Reviews* 32 (2):234–58.
889 https://doi.org/10.1111/j.1574-6976.2008.00105.x.
890 Sawa, Justyna, Hélène Malet, Tobias Krojer, Flavia Canellas, Michael Ehrmann, and Tim
891 Clausen. 2011. “Molecular Adaptation of the DegQ Protease to Exert Protein Quality
892 Control in the Bacterial Cell Envelope.” *Journal of Biological Chemistry* 286
893 (35):30680–90. https://doi.org/10.1074/jbc.M111.243832.
894 Shah, Devang, Zhigang Zhang, Arkady Khodursky, Niilo Kaldalu, Kristi Kurg, and Kim
895 Lewis. 2006. “Persisters: A Distinct Physiological State of *E. coli*.” *BMC Microbiology*
896 6 (53). https://doi.org/10.1186/1471-2180-6-53.
897 Shan, Yue, Autumn Brown Gandt, Sarah E. Rowe, Julia P. Deisinger, Brian P. Conlon, and
898 Kim Lewis. 2017. “ATP-Dependent Persister Formation in *Escherichia coli*.” *mBio* 8
899 (1):e02267-16. https://doi.org/10.1128/mBio.02267-16.
900 Shaner, Nathan C., Robert E. Campbell, Paul A. Steinbach, Ben N.G. Giepmans, Amy E.

Palmer, and Roger Y. Tsien. 2004. “Improved Monomeric Red, Orange and Yellow Fluorescent Proteins Derived from *Discosoma* Sp. Red Fluorescent Protein.” *Nature Biotechnology* 22 (12):1567–72. https://doi.org/10.1038/nbt1037.

Shapiro, Howard M. 2000. “Membrane Potential Estimation by Flow Cytometry.” *Methods* 21 (3):271–79. https://doi.org/10.1006/meth.2000.1007.

Sklar, Joseph G., Tao Wu, Daniel Kahne, and Thomas J. Silhavy. 2007. “Defining the Roles of the Periplasmic Chaperones SurA, Skp, and DegP in *Escherichia coli*.” *Genes and Development* 21 (19):2473–84. https://doi.org/10.1101/gad.1581007.

Takeuchi, Shoji, Willow R. Diluzio, Douglas B. Weibel, and George M. Whitesides. 2005. “Controlling the Shape of Filamentous Cells of *Escherichia coli*.” *Nano Letters* 5 (9):1819–23. https://doi.org/10.1021/nl0507360.

Tripathi, Arti, Pooja C. Dewan, Shahbaz A. Siddique, and Raghavan Varadarajan. 2014. “MazF-Induced Growth Inhibition and Persister Generation in *Escherichia coli*.” *Journal of Biological Chemistry* 289 (7):4191–4205. https://doi.org/10.1074/jbc.M113.510511.

Verstraeten, Natalie, Wouter Joris Knapen, Cyrielle Ines Kint, Veerle Liebens, Bram Van den Bergh, Liselot Dewachter, Joran Elie Michiels, et al. 2015. “Obg and Membrane Depolarization Are Part of a Microbial Bet-Hedging Strategy That Leads to Antibiotic Tolerance.” *Molecular Cell* 59 (1):9–21. https://doi.org/10.1016/j.molcel.2015.05.011.

Völzing, Katherine G., and Mark P. Brynildsen. 2015. “Stationary-Phase Persisters to Ofloxacin Sustain DNA Damage and Require Repair Systems Only during Recovery.” *mBio* 6 (5):e00731–46. https://doi.org/10.1128/mBio.00731-15.

Waller, Patrick R.H., and Robert T. Sauer. 1996. “Characterization of *DegQ* and *DegS*, *Escherichia coli* Genes Encoding Homologs of the DegP Protease.” *Journal of Bacteriology* 178 (4):1146–53. https://doi.org/10.1128/jb.178.4.1146-1153.1996.

Wang, Xiaoxue, and Thomas K. Wood. 2011. “Toxin-Antitoxin Systems Influence Biofilm and Persister Cell Formation and the General Stress Response.” *Applied and Environmental Microbiology* 77 (16):5577–83. https://doi.org/10.1128/AEM.05068-11.

Wilks, Jessica C., and Joan L. Slonczewski. 2007. “pH of the Cytoplasm and Periplasm of *Escherichia coli*: Rapid Measurement by Green Fluorescent Protein Fluorimetry.” *Journal of Bacteriology* 189 (15):5601–7. https://doi.org/10.1128/JB.00615-07.

Wilmaerts, Dorien, Mariam Bayoumi, Liselot Dewachter, Wouter Knapen, Jacek T Mika, Johan Hofkens, Peter Dedecker, Giovanni Maglia, Natalie Verstraeten, and Jan Michiels. 2018. “The Persistence-Inducing Toxin HokB Forms Dynamic Pores That Cause ATP Leakage.” *mBio* 9 (4):e00744-18. https://doi.org/10.1128/mBio.00744-18.

Wilmaerts, Dorien, Etthel M. Windels, Natalie Verstraeten, and Jan Michiels. 2019. “General Mechanisms Leading to Persister Formation and Awakening.” *Trends in Genetics*. Elsevier Ltd, 1–11. https://doi.org/10.1016/j.tig.2019.03.007.

Zwietering, M. H., I. Jongenburger, F. M. Rombouts, and K. Van’t Riet. 1990. “Modeling of the Bacterial Growth Curve.” *Applied and Environmental Microbiology* 56 (6):1875–81. https://doi.org/10.1111/j.1472-765X.2008.02537.x.